Effect of an axial jet on vortex merging

David Marles and Ismet Gursul
Department of Mechanical Engineering, University of Bath, Bath BA2 7AY, United Kingdom

(Received 13 June 2007; accepted 28 February 2008; published online 21 April 2008)

Experiments were conducted to understand the effect of an axial jet on the merging process of a simulated flap-edge and wing-tip corotating vortex pair in the near wake. Cross-flow velocity measurements and flow visualization were performed for the three realistic jet positions on both equal and unequal strength like-signed vortices for a range of momentum coefficients. The main finding was that the initial jet position has a vastly contrasting effect on the merging process. If the jet turbulence rapidly interacts with only one of the vortices, severe diffusion of that vortex occurs which ultimately wraps around and becomes consumed by the unaffected vortex structure. The jet causes a reduction in the vortex spacing and an increase in the rotation angle; hence, merging is promoted. If the jet turbulence does not directly interact with either vortex but instead interferes with the mechanism in the outer-recirculation region that advects vorticity to a larger radius, then merging can be retarded. In this case, an increase in vortex spacing and reduction in rotation angle were observed. Increasing the momentum coefficient, hence, introducing more turbulence into the flow, has a greater effect on the merging process. © *2008 American Institute of Physics*.
[DOI: 10.1063/1.2907210]

I. INTRODUCTION

Wakes generated by lifting aircraft wings consist of spanwise vorticity sheets that rapidly roll up into distinct vortex structures.[1] The exact configuration of the lifting surface governs the strength and number of vortices produced. Cruise conditions generate a pair of discrete counter-rotating vortices at the extremities of the wings. During low speed flight, which occurs in close proximity to airfields, lift augmentation devices are deployed. A corotating vortex pair emanates from the flap-edge and wing-edge tips which subsequently merge into a single vortex within a downstream distance x of 5–10 spans, resulting in a wake structure similar to that during cruise.[2] These vortices pose a serious hazard to trailing aircraft and limit airport capacity due to their longevity.

The fluid dynamics of vortex merging has recently received renewed enthusiasm due to its applicability to the decay of two-dimensional turbulence, three-dimensional turbulence, and mixing layers. For the purpose of this article, its relevance to aircraft wakes will be discussed. Depending on the particular setting of the high lift devices, equal and unequal strength corotating vortices can be generated which is an important factor in the merger process. Vortices of comparable strength undergo a symmetric merger which takes place at the extremities of the vortex. For an unequal strength pair, the stronger vortex dominates the dynamics, radially splitting the weaker structure with severity depending on their relative strengths.[3] For large differences in strength, catastrophic merger very rapidly occurs as the weaker vortex is first axially split, then wrapped around the dominant vortex.

Previously, vortex merging of equal strength like-signed vortices has been divided into three distinct stages[4] with Cerretelli and Williamson[5] adding a fourth to describe a second diffusion stage of the vortices at the end of merging. Merging is a two-dimensional laminar process at Reynolds number based on circulation ($\mathrm{Re}_\Gamma=\Gamma/\nu$) less than $\mathrm{Re}_\Gamma \approx 2000$, where Γ is the circulation and ν is the kinematic viscosity. The vortex cores rotate due to their mutually induced velocity. Numerical simulations performed by Leweke *et al.*[6] on Lamb–Oseen vortices with a Gaussian vorticity profile demonstrated that the merging was initiated when the core radius a to separation distance h ratio exceeded the critical value of $a/h=0.25\pm0.01$. Experiments revealed that the merger commenced once the time-dependent core exceeded approximately 29% of the vortex separation distance for low Reynolds number flow.[4,5,7] Recently, Meunier *et al.*[8] suggested this value to be slightly over predicted, proposing a merging criterion $a/h=0.24\pm0.01$ from experimental results. Inviscid simulations show no merger if the ratio a/h is less than the critical value. The vortex pair will indefinitely rotate around each other at a fixed separation. However, viscous diffusion in real flows always causes merger as a result of the growth of the vortex cores. This initiates the second stage known as the convective phase in which the separation distance of the pair decreases. Arms of vorticity are radially ejected outward as a result of the fluid being advected by the outer-recirculation region. The antisymmetric vorticity field generated induces an inward velocity that drives the vortex cores together.[5] Alternatively, this idea can be viewed as the spiral arms cause the approach of the vortex cores to conserve angular momentum.[2] As the vortex spacing approaches zero, the inward induced velocity applied to the cores becomes negligible. This leaves the vortices at a spacing to be approximately equal to 20% of the initial separation according to Cerretelli and Williamson.[5] The resulting pair of close vorticity peaks matures into a single core by a second diffusive stage. The structure is transformed into an approximate

axisymmetric vortex with about twice the area of the original individual vortices.[4,6]

The phenomenon of instabilities occurring between a pair of vortices is well documented. Long-wavelength and shorter-wave elliptical instabilities have been observed in counter-rotating vortices by Crow[9] and Leweke and Willamson,[10] respectively. For corotating vortices, the longer-wavelength Crow-type instability is known to be suppressed by the rotation of the vortex pair.[11] Recently and for the first time, Meunier and Leweke[4] observed that corotating vortices with prolonged diffusive periods (diffusive stage is proportional to Reynolds number) exhibited elliptical instabilities. This occurs for Reynolds number greater than $\mathrm{Re}_\Gamma \approx 2000$ or small initial core size to vortex spacing, allowing time for the growth of three-dimensional instabilities. Experiments performed by Meunier *et al.*[2] revealed that three-dimensional merger can be initiated earlier (in terms of viscous time period), for core sizes as low as 19% of the vortex separation, even though the entire merger process may actually take longer (in terms of convective units, $t_0 = 2\pi^2 h^2/\Gamma$, for two point vortices of the same strength). The instability causes sinusoidal distortion of the vortex centerline with a wavelength similar to the vortex separation. This deformation aids the transfer of vorticity across the separatrices, allowing the outer-recirculation region to advect this fluid to a larger radius. Another effect of merging involving elliptical instabilities is that the final merged vortex has a core area of 3.5 times that of the unmerged pair. In contrast, two-dimensional merger only produces approximately 1.5–2.0 times the area increase, resulting in a more concentrated vortex core with larger peak vorticity.[2,4] This has the effect of increasing the maximum azimuthal velocity of the final vortex by approximately 1.5 times over the case where instabilities were present.

Extensive experimental and numerical studies have been performed on the interaction of a jet with a single vortex.[12] Research revealed that there are two types of interaction depending on the initial distance between the jet and vortex. For small initial jet-vortex spacing, similar to a Batchelor q vortex,[13] strong injection of axial perturbations into the core causes severe diffusion of the vortex structure.[14] This arrangement is analogous to an engine located close to a flap edge on aircraft with four engines. Interactions for larger initial jet-vortex spacing has a vastly different flow topology. Findings reveal that the wake development can be divided into two phases. The first of these, known as the jet regime, sees the simultaneous turbulent mixing of the jet with ambient fluid and roll up of the wing-generated vorticity sheet around discrete vortices. Jet growth is known to be dominated by the Kelvin–Helmoltz-type instability which has been studied by Michalke and Herman[15] for a simple inviscid incompressible axisymmetric jet. For numerical simulations, it is assumed that minimal interaction occurs between the jet and the vortex during this stage.[14] The next phase, known as the interaction regime, is dominated by the entrainment of the jet around the vortex. Interaction between the jet axial and vortex tangential velocities causes secondary vortices to be generated around the periphery of the vortex.

Wang *et al.*[16] performed experiments on a coflowing jet immersed in an induced velocity field which was generated by the vortex wake of a delta wing. The jet was significantly modified by the vortices, losing its axisymmetric shape and undergoing vertical compression and lateral stretching. However, little effect was observed on the trajectory of the vortices. Further experiments performed by Wang and Zaman[17] revealed the presence of additional vortical structures of significant strength around the jet. These secondary vortices are the mechanism responsible for the deformation of the jet structure which ultimately results in a more rapid decay in maximum axial velocity. Margaris *et al.*[18] performed a parametric study on the effect of a coflowing jet on a single wing-tip vortex. The jet turbulence was observed to elongate and wrap around the vortex, producing a more diffuse vortical structure with reduced levels of both vorticity and cross-flow velocity. Smaller initial jet-vortex separations and larger momentum coefficients allowed a more rapid ingestion of the turbulence into the vortex, which had the greatest effect on the coherence of the vortical flow.

The objective of the present paper is to provide an insight into the effect of jet turbulence on corotating vortex merger in the near wake. Extensive simulations and experiments have been performed on the merger process, which is now relatively well understood. However, there remains a large void in the knowledge of cold engine jet interaction and its effect on the merging process. This study uses a pair of generic rectangular wings to generate a vortex pair and a round nozzle to simulate the coflowing engine exhaust. Both equal and unequal strength vortices were produced to replicate aircraft with lift augmentation devices deployed. The initial jet nozzle position relative to the vortices was varied along with the vortex separation distance.

II. EXPERIMENTAL SYSTEM AND TECHNIQUES

A. Experimental setup

1. Facilities and models

Experiments were conducted in an Eidetic model 1520 closed circuit free surface water tunnel at the University of Bath. The corotating vortex pair was generated by using generic rectangular wings vertically suspended (Fig. 1) in the $0.381 \times 0.508 \times 1.524$ m^3 test section. This produced a submerged semispan $s = 230$ mm and aspect ratio of 11.5 (based on the full span). All experiments were performed with a free stream velocity, $U_\infty = 0.3$ m s^{-1} on 5% cambered airfoils with chord, $c = 40$ mm. The aluminum wings were of constant thickness of 5% chord with rounded leading and trailing edges. This provided a Reynolds number based on chord, $\mathrm{Re} = U_\infty c/\nu$ of 12 000. Florescent dye was introduced into the vortices by using a 0.5 mm tube embedded in the pressure surface of the wings. Engine exhaust flux was simulated via a round nozzle aligned with the free stream having an exit diameter $d_j = 6$ mm and a 0.5 mm wall thickness. The nozzle support was U shaped to minimize interference allowing the jet to be located between the vortex generating wings. A constant diameter, 40 mm long straight section extending from the support released the jet fluid in the same cross-flow plane as the trailing edges of the generic wings (Fig. 1). The dye was introduced into the jet via a 1 mm tube located in

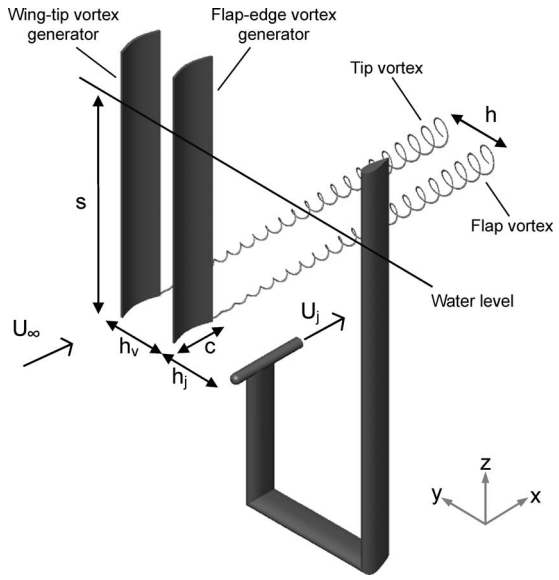

FIG. 1. Schematic of generic wings and jet nozzle model.

the nozzle support structure. Measurements were taken at numerous cross-flow planes downstream of the model between $x/c=4$ and 24, measured from the trailing edge of the wings, as illustrated in Fig. 2.

2. Instrumentation

Quantitative measurements were obtained by using a two-dimensional TSI digital particle image velocimetry (PIV) system which produces up to 120 mJ pulses from a pair of mini Nd:YAG (yttrium aluminum garnet) laser heads at a rate of 3.75 pairs/s. Images were taken with an 8 bit gray scale 2048×2048 pixel digital charge coupled device camera. The tunnel was seeded with hollow glass spheres of $8-12$ μm mean diameter. Cross correlation was performed on 100 image pairs by using Hart algorithm with a 32×32 pixel interrogation window and 50% overlap. This produced a vector spatial resolution at the measurement stations $x/c=4$ and 24 of approximately 4% and 2% of the chord length, respectively. Uncertainty in the velocity data was estimated to be 2%.

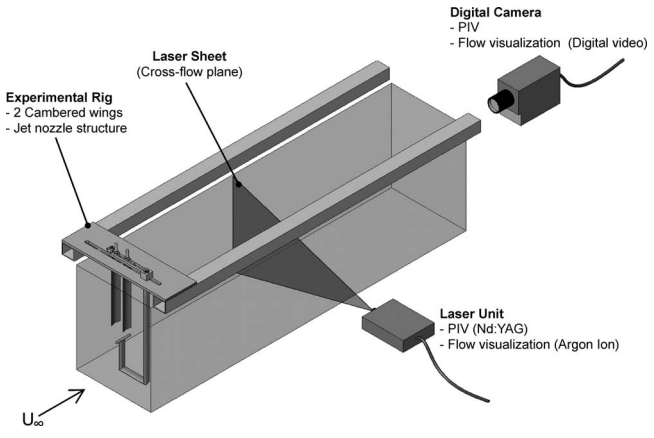

FIG. 2. Experimental setup in water tunnel.

Flow visualization was achieved by illuminating the fluorescent dye via a Coherent Innova70 4 W continuous emission argon-ion laser, emitting a 515 nm wavelength beam. Green (rhodamine 6G) and red (rhodamine B 500%) dyes were used to distinguish between the vortex and jet flows, respectively. Instantaneous images were extracted from video footage recorded at a rate of 25 frames/s.

B. Data analysis

Detailed analysis of the merging process requires each vortex to be isolated from the surrounding vorticity field. This requires accurate vortex center positions to be found. An initial approximation for the two center locations was made by finding their corresponding peak vorticity values. The flow field was then separated perpendicular to a line connecting the vortex centers. The division occurred at the point of minimum vorticity between the vortices. This approach is reasonably reliable for axisymmetric vorticity distributions. However, vortex merger in conjunction with the diffusion generated by jet turbulence produces elongated vorticity structures. This results in a time-averaged field with no clearly defined vorticity peak, making this method unpredictable. The problem was overcame by first dividing the field using the approximate vorticity peaks, as discussed above, and then calculating the vorticity centroid for each vortex patch as documented by Chen *et al.*[3] The two-dimensional centroid positions, y_c and z_c, are found by considering the vorticity distribution in the y and z directions,

$$y_c = \frac{1}{\Gamma}\iint y\omega dydz, \tag{1}$$

$$z_c = \frac{1}{\Gamma}\iint z\omega dydz, \tag{2}$$

where ω is axial vorticity, y is the outboard direction along the span, and z is the normal direction upwards. For this method to accurately and consistently work, vorticity with an absolute value less than 5% of the maximum was removed. This prevented background noise with large moment arms having a major influence on the centroid location.

Downstream development of the pair produces a flow field that consists of elongated patches of vorticity. Additional diffusion of one or both vortices by jet turbulence makes the process of deciding whether a vorticity patch has merged into a single structure very subjective. In an attempt to remove any ambiguity and make the process quantitative, the following procedure was performed. First, the peak vorticity of the entire field was found; this supplies the approximate center location of the more dominate vortical structure. A second point was found by using the vorticity centroid for the entire field. Comparison of these two positions provides a measure of the extent of merging. If the two points coincide, then there is a single axisymmetric vorticity distribution in the flow. If these two points are different, then this indicates that the pair is unmerged. This is because the vorticity patch from the second vortex tends to attract the centroid. To automate the process, a criterion was applied to classify merged and unmerged vortices. If the difference between the vortic-

TABLE I. Aircraft parameters.

Aircraft	Span (m)	Flap span/wing span ratio	Chord (mean aerodynamic) (m)	Number of engines	h_v/c
A330-300	58.0	0.665	7.26	2	1.34
B757-300	38.1	0.757	5.64	2	0.82
A340-500	61.2	0.625	8.35	4	1.37
B747-400	62.3	0.639	9.68	4	1.16

ity centroid and peak vorticity positions for the entire field was $\geqslant 0.05c$, then the flow contains unmerged vortices. This criterion was produced from observation made on the vorticity field and is approximately equivalent to 17% of a vortex core diameter. If the vortices were unmerged, the field was divided into two and the vorticity centroid for each vortex was found as detailed above. If the vortices were merged, therefore, only containing a single vortical structure, then the vorticity centroid for the entire field was used to find the vortex center.

Circulation was then determined by performing a line integral of the velocities around a closed loop on each isolated vortex to calculate their relative strengths. The integration path was incrementally expanded around the vortex center until the resulting circulation value reached an asymptotic maximum. The sum of the circulation for the flap and tip gave the total circulation for the entire flow field, $\Gamma_0=\Gamma_t+\Gamma_f$. Similar to the work of Chen *et al.*,[3] the integration paths for each do not overlap.

The turbulence produced in the wake was calculated by taking the standard deviation of cross-flow velocities U_{std}. This term is a little misleading because the low frame rate PIV system does not give the true turbulence data. However, this is sufficient to provide information on the magnitude and location of the largest fluctuations in the cross-flow velocity field.

III. RESULTS

A. Experimental parameters

The present setup generates a pair of vortices by using two cambered aerofoils. This arrangement is not identical to that of real wings but the trailing vortical field created mimics that of an aircraft with high lift devices deployed. This experimental setup offers greater flexibility as the initial vortex spacing h_v and jet-vortex spacing h_j can be altered with ease (Fig. 1). The separation distance was a compromise between minimizing interference between the aerofoils and ensuring that merger will occur within the length of the water tunnel test section. The coordinate system is based on the effective starboard aircraft wing being represented by the model in Fig. 1. The trailing edge tip of the effective wing is taken as the origin, in other words, the trailing edge tip of the wing generating the tip vortex. For this investigation, the main spacing between the vortices was $h_v/c=0.75$ with some additional testing performed at $h_v/c=1.0$. Table I reveals how these values compare with the spacing taken from real aircraft configurations.

Realistic momentum coefficients were taken from the work of Margaris *et al.*[18] who supply a comprehensive analysis of vortex strength to jet flux ratio for real aircraft configurations. Experiments were performed for axial jet exit velocities, U_j normalized by the free stream velocities $U_j/U_\infty=0$, 2.01, 2.85, and 4.03 which correspond to momentum coefficients $C_\mu=0$, 0.025, 0.05, and 0.1 (based on a single vortex generating wing). Momentum coefficient is defined as

$$C_\mu = \frac{\rho_j A_j U_j^2}{\frac{1}{2}\rho_\infty U_\infty^2 cs}, \tag{3}$$

where ρ_j and ρ_∞ are the densities of the jet and free stream fluid, respectively, A_j is the exit area of jet nozzle and s is the semispan (submerged span) of the aerofoil. Their data show that a minimum initial spacing of $h_j/c=0.6$ ensures the least interference effects from the jet nozzle structure. The jet was located in three positions relative to the vortex generating wings. These were chosen for their physical similarity to real aircraft designs. Table II provides a description of these positions along with a schematic of the experimental arrangement and effective real aircraft geometry being modeled. Configuration I represents the approximate jet/vortex positioning for aircraft with two engines such as the A330 or B757. The outboard engines on four engined aircraft are modeled in configurations II and III which represent the A340 and B747, respectively.

Both equal and unequal strength corotating vortices were generated in an attempt to model a realistic aircraft wake structure. For an equal strength pair, the wings were set at an angle of attack $\alpha=10°$. This produced a circulation ratio for the flap and tip vortices $\Gamma_f/\Gamma_t=1.06$ at $x/c=4$ with no jet nozzle structure in the flow and Reynolds number based on circulation $\text{Re}_\Gamma=6500$ (for a single vortex). Assuming that the vortex radius a is taken as the distance from the vortex center to maximum tangential velocity at $x/c=4$ with no nozzle in the flow, we estimate a radius to separation ratio $a/h\approx 0.2$. For the purposes of this paper, it is assumed that the physical spacing of the generic wing tips is equal to the initial vortex spacing. Likewise, the jet-to-flap separation is assumed to be synonymous with the initial jet-to-vortex spacing. Throughout the paper, the vortices will be referred to as the flap and the tip, which correspond to the flap-edge and wing-tip vortices, respectively. Cross-flow measurements were taken at four chord length intervals which equate to a normalized orbit time $t^*=t/t_0$ of 0.19 where t is time. Unequal strength vortices occur when the high lift devices are configured for takeoff and landing flight regimes, having circulation ratios $\Gamma_f<\Gamma_t$ and $\Gamma_f>\Gamma_t$, respectively. Setting the angles of attack for the flap and the tip to $\alpha_f=10°$, $\alpha_t=5°$ and $\alpha_f=5°$, $\alpha_t=10°$ produced unequal strength vortices with ratios $\Gamma_f/\Gamma_t=1.54$ and 0.65, respectively, at the most upstream measurement location.

TABLE II. Summary of the experimental setup and effective aircraft arrangement being modeled. Schematic views are looking upstream in the water tunnel for a starboard aircraft wing.

Configuration	Description	Experimental Arrangement			Effective Aircraft Configuration
		h_v/c	h_j/c	Setup	
I	Jet in same spanwise plane as flap-edge and wing-edge tips	0.75 1.0	0.6	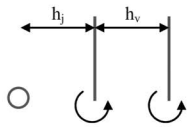	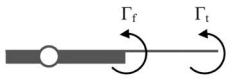
II	Jet vertically below flap-edge tip	0.75 1.0	0.6	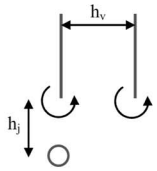	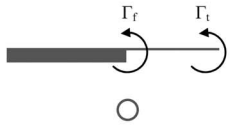
III	Jet vertically below center of flap-edge and wing-edge tips	1.0	0.6	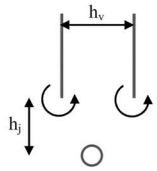	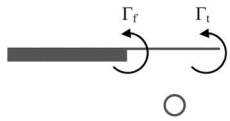

B. Equal strength vortex merging

Flow visualization was performed to illustrate the interaction between the jet and the vortex pair as they develop downstream. Figure 3 compares the results for two different jet positions which both have the same initial vortex spacing $h_v/c=0.75$. The left and right columns contain visualization images for the nozzle center being located on a horizontal line inboard of the flap (configuration I) and beneath the flap (configuration II), respectively.

Figures 3(a)–3(c) show the downstream development of the vortex pair from $x/c=4$ to 24 with the nozzle in configuration I and jet flux $C_\mu=0.025$. The jet fluid is observed to become rotated and stretched by the flow field generated by the vortex pair. However, the counterclockwise rotation rate of the vortices appears to be greater than that of the jet fluid. It emerges that moving downstream, the jet slowly interacts with the vortices. At the greatest distance downstream, there are still two distinct vortex structures, suggesting that merging is not complete.

Positioning the jet vertically below the flap [Figs. 3(d)–3(f)], produces a vastly different interaction between the jet and vortex structures from that observed in Figs. 3(a)–3(c). It is clear that at $x/c=4$, the jet fluid has been elongated and wrapped around the flap vortex. Reasoning for this is probably because the rotation of the vortex pair tends to move the flap vortex into the path of the jet flux. Moving further downstream causes the tip vortex to wrap the jet fluid around itself. The images reveal that at $x/c=24$, there appears to be a single merged structure where the remnants of the jet fluid have been rolled up around the solitary vortex. Hence, the flow visualization reveals that the jet alters the development of the flap and tip vortices when comparing the two nozzle configurations. It appears that configuration I has a reduced rate of rotation compared to configuration II. At $x/c=24$, this difference is clearly visible because the spanwise jet location [Fig. 3(c)] demonstrates an unmerged vortex pair, whereas configuration II [Fig. 3(f)] promotes the production of a single axisymmetric merged structure.

Figures 4 and 5 show the jet effect on vortex merger by using contours of time-averaged axial vorticity as a function of momentum coefficient. At $x/c=16$, the reference case with no nozzle in the flow can be seen in Fig. 4(a). The vortices at this station have become slightly elongated, an expected result of being close to merging. Introducing the nozzle structure at $h_j/c=0.6$ horizontally from the flap, as in Fig. 4(b), clearly has an effect on the merging process. A reduction in rotation angle and a small break in the lowest level vorticity contour between the pair suggest a delay in merger. This trend is continued as momentum coefficients are increased to $C_\mu=0.025$, 0.05, and 0.1 in Figs. 4(c)–4(e), respectively. Clearly the jet turbulence has retarded merger, causing an increase in separation distance and decrease in the angle that the pair has rotated through. From the conservation of momentum, a change in separation will be accompanied by an adjustment in the rate of rotation. Increasing momentum flux produces a more diffuse flap vortex, while the tip vortex becomes more concentrated.

Vorticity contours for the jet vertically below the flap (configuration II) can be found in Fig. 5. The measurement station has been moved upstream to $x/c=8$ because it appears that the jet in this configuration promotes merger; hence, only a single vortex exists further downstream. The reference case with no nozzle in the flow [Fig. 5(a)] shows two discrete vortex structures that are far from merging. Introducing the jet nozzle in Fig. 5(b) causes the approach of the vortex pair and a small increase in rotation angle.

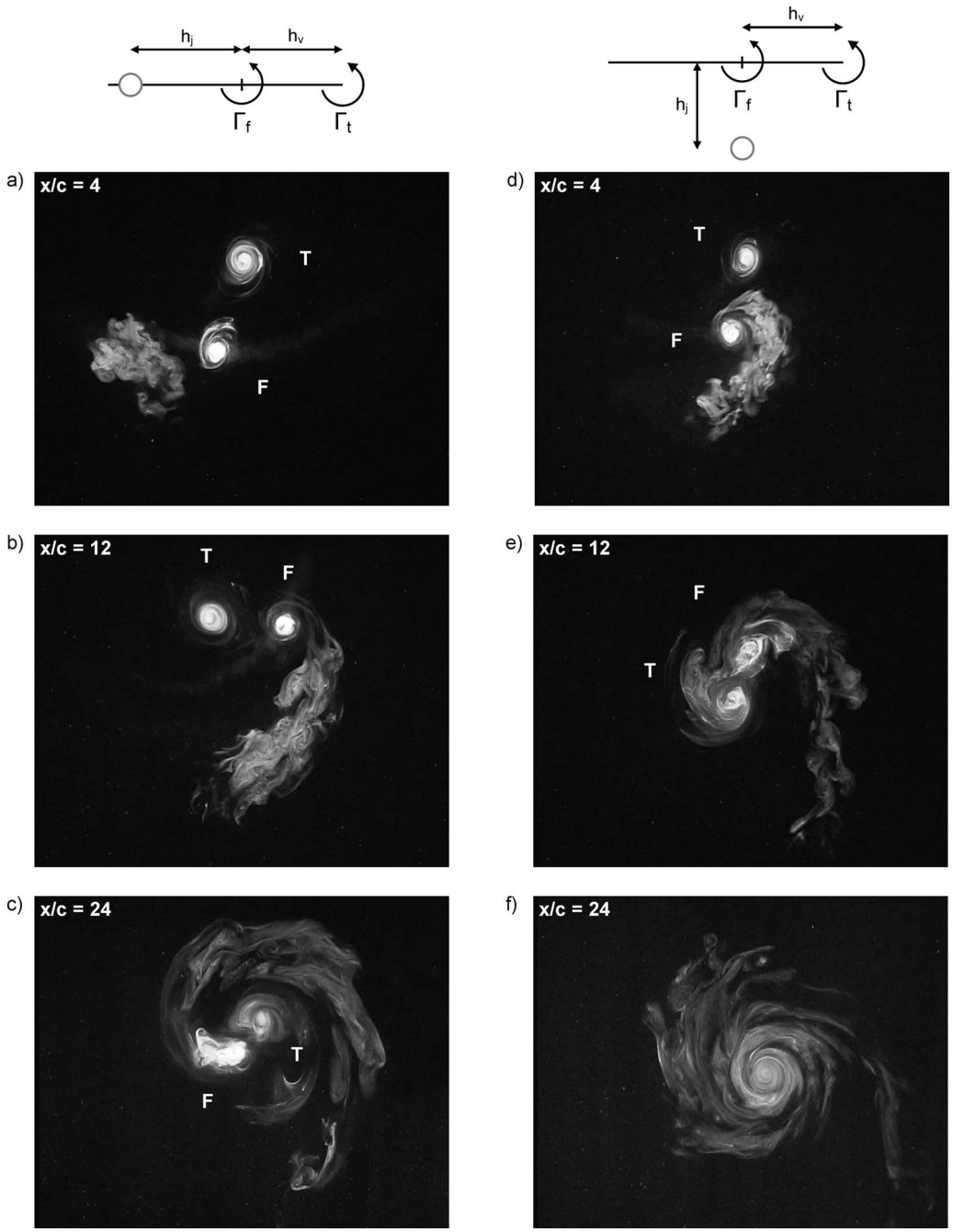

FIG. 3. Flow visualization for equal strength corotating vortices (T=tip vortex, F=flap vortex), $h_v/c=0.75$, $h_j/c=0.6$, and $C_\mu=0.025$. Left column, configuration I and right column, configuration II. Schematic illustrates the experimental setup.

Figure 5(c) reveals the effect of increasing the jet flux to $C_\mu=0.025$. Clear diffusion of the flap vortex occurs as the still high intensity jet turbulence rapidly interacts with this vortex, as illustrated by the flow visualization in Fig. 3(d). In addition, the tip vortex appears to succumb to the jet turbulence, causing a slight diffusion. Interaction of the jet turbulence with the tip vortex was also observed in the flow visualization at $x/c=12$. Increasing the strength of the jet to $C_\mu=0.05$ and 0.1 in Figs. 5(d) and 5(e), respectively, reveals how effective the jet is at diffusing the flap vortex. The results suggest that the more diffuse flap vortical structure begins to stretch and wrap around the more concentrated tip vortex. The lower levels of vorticity around the edge of a diffuse vortex can be removed in a process known as strain-induced vortex stripping as documented by Dritschel.[19] It appears that the jet flux reduces the separation distance, increases the rotation angle, and causes significant diffusion of the flap vortex. Another explanation comes from the idea that unequal strength vortices more rapidly merge than if they were of equal strength.[3] However, it should be noted that there was a negligible difference in circulation of around 0.5% when comparing the $C_\mu=0$ and 0.1 cases.

To confirm whether the changes in peak vorticity in the time-averaged field for configuration I are a function of vortex wandering or an actual reduction in vorticity, instantaneous data were analyzed. Figure 6 illustrates the instanta-

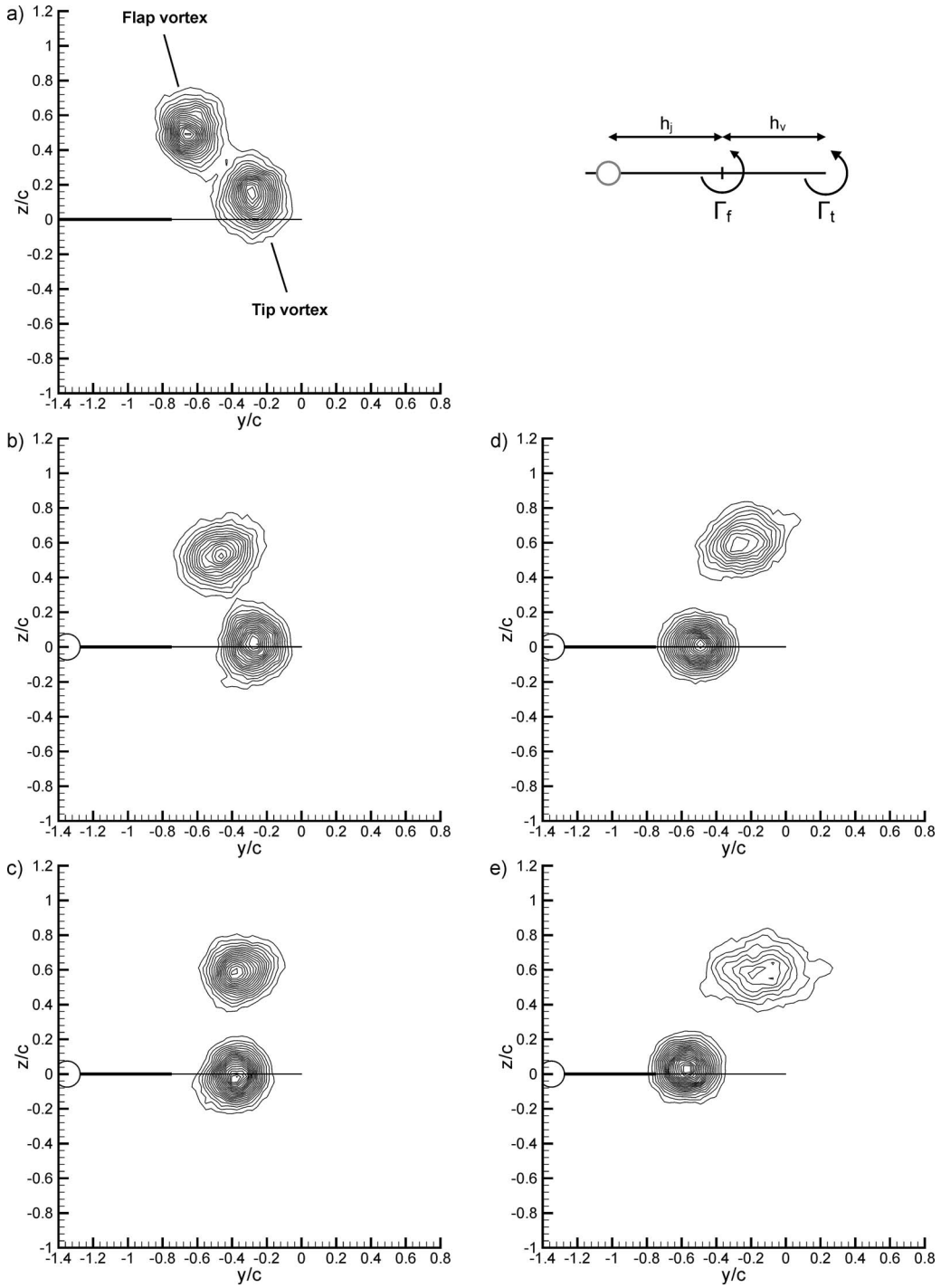

FIG. 4. Normalized vorticity for equal strength corotating vortices at $x/c=16$, $h_v/c=0.75$, and $h_j/c=0.6$. (a) Reference case (no nozzle in flow), (b) $C_\mu=0$, (c) 0.025, (d) 0.05, and (e) 0.1. Minimum contour level $\omega c/U_\infty=0.5$ with 0.25 intervals. Schematic illustrates the experimental setup (configuration I).

neous peak vorticity location for each vortex along with the standard deviation of the vortex positions plotted as error bars at the time-averaged center location. Comparing Figs. 6(a) and 6(b), it is clear that introducing the nozzle into the flow significantly increases the wandering of the flap vortex in the spanwise direction. Increasing momentum flux to $C_\mu=0.025$ reduces the wandering of both vortices [Fig. 6(c)], perhaps because the pair moves away from a merged condition. Increasing the momentum coefficient further sees a major reduction in the time-averaged peak vorticity (Fig. 4). For a $C_\mu=0.1$ [Fig. 4(d)], there is an approximately 60% reduction in maximum vorticity when compared to the time-averaged reference case [Fig. 4(d)]. This large reduction is probably due to the severe wandering of the flap vortex in Fig. 6(e). In addition, the wandering amplitude of the flap vortex was found to increase with downstream distance. Similar increases in wandering of a single trailing vortex as a result of the introduction of jet turbulence has been observed by Margaris *et al.*[18] The tightening of the tip vortex visible in Fig. 4 as the momentum coefficient increases has been attrib-

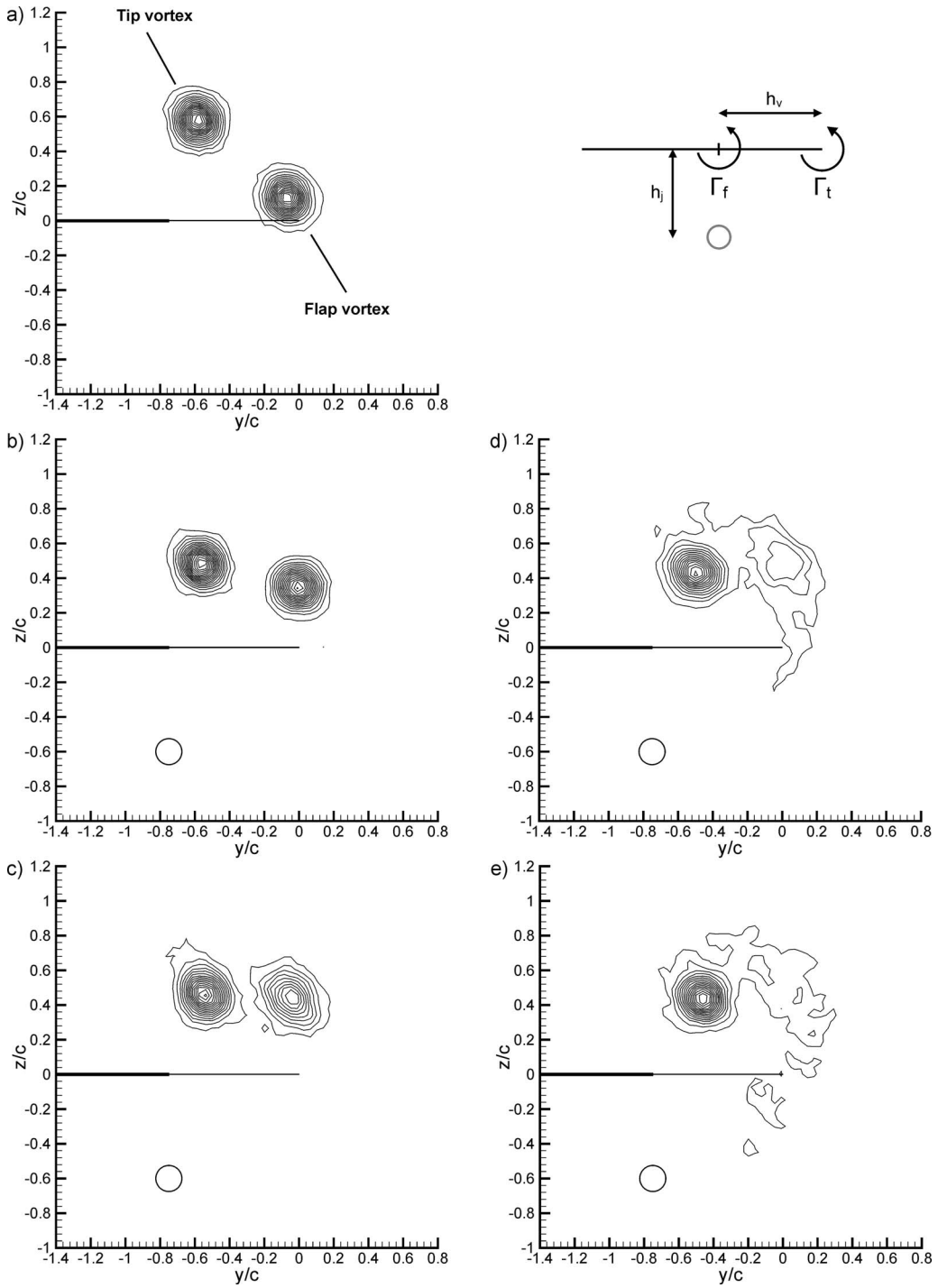

FIG. 5. Normalized vorticity for equal strength corotating vortices at $x/c=8$, $h_v/c=0.75$, and $h_j/c=0.6$. (a) Reference case (no nozzle in flow), (b) $C_\mu=0$, (c) 0.025, (d) 0.05, and (e) 0.1. Minimum contour level $\omega c/U_\infty=0.5$ with 0.5 intervals. Schematic illustrates the experimental setup (configuration II).

uted to a reduction in wandering which is visible in Fig. 6. This is believed to occur because the pair moves further away from a merged state.

Figures 7 and 8 illustrate the vortex pair spacing and rotation angle as they progress downstream for the horizontal and vertical jet configurations, respectively. Concentrating on the horizontal jet with no nozzle in the flow, Fig. 7(a) shows an approximately constant rate of rotation to just over 360° or one orbit. Figure 7(b) follows this trend with the pair approaching each other at an approximate linear rate up to $x/c=20$. The data terminate at this point because for the next measurement station, $x/c=24$, only a single vortex exists. The dashed line represents the collapse of the vortex pair into a single structure. There appears to be only a very small diffusive period because a reduction in vortex spacing immediately occurs at $x/c=4$. This suggests that the convective merger stage is active which is possible because the pair has fulfilled the criterion required for the production of three-dimensional instabilities during the merger, that is, at the upstream measurement location $(x/c=4)$ $a/h\approx0.2$ and

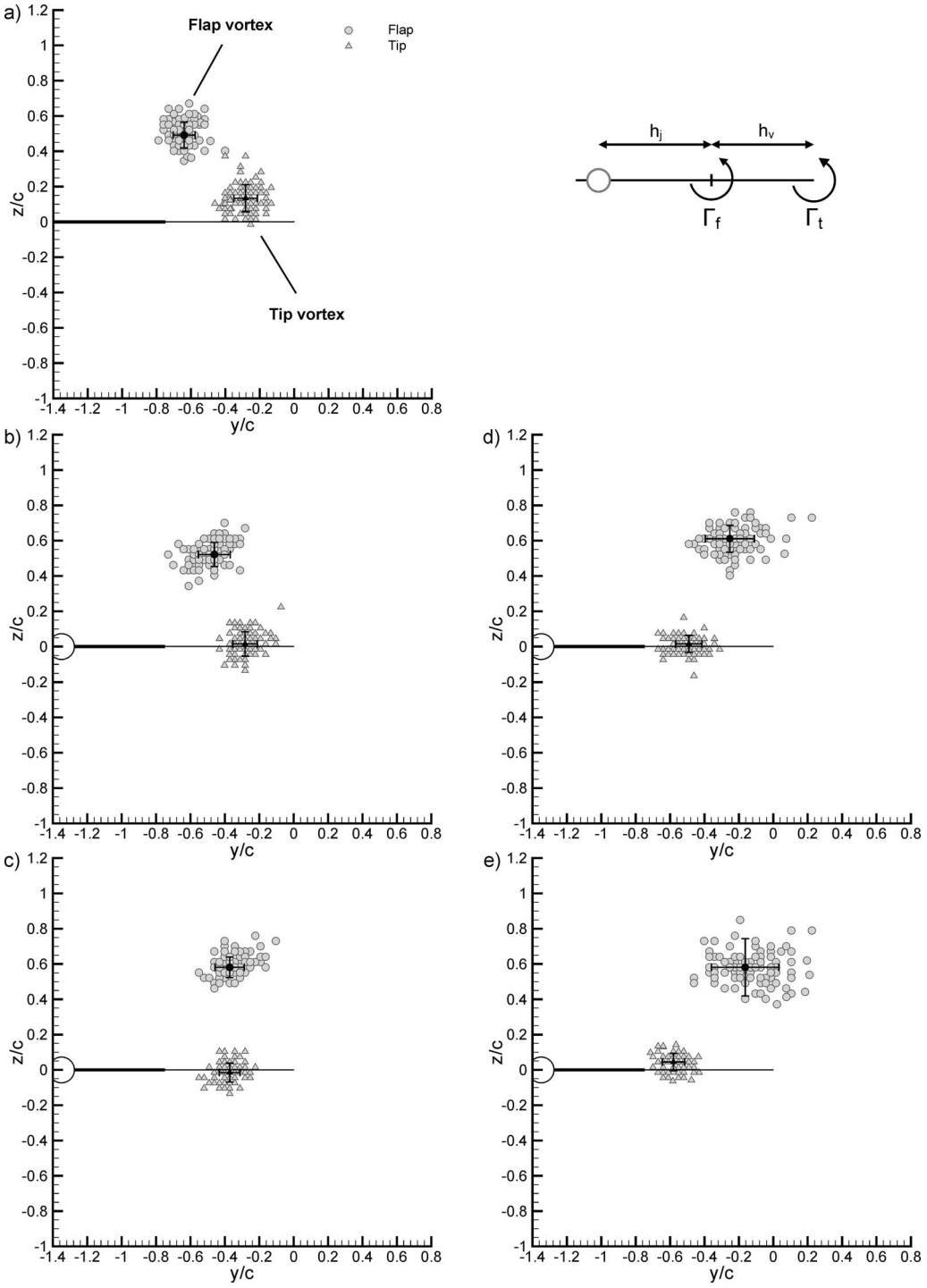

FIG. 6. Instantaneous peak vorticity locations for equal strength corotating vortices at $x/c=16$, $h_v/c=0.75$, and $h_j/c=0.6$ with the jet in configuration I (see schematic). Error bars represent the standard deviation of positions about the time-averaged center location. (a) Reference case (no nozzle in flow), (b) $C_\mu=0$, (c) 0.025, (d) 0.05, and (e) 0.1.

$\mathrm{Re}_\Gamma > 2000$. Another indication that elliptical instabilities are present is revealed when assessing the increase in vortex size as a result of merging. The radius at the most upstream measurement station for a single unmerged vortex is $a_{\mathrm{initial}}/c \approx 0.13$. At the most downstream location, the radius of the single merged axisymmetric vortex is $a_{\mathrm{final}}/c \approx 0.24$. This corresponds to an increase in area of $(a_{\mathrm{initial}}/a_{\mathrm{final}})^2 \approx 3.5$, which is consistent with the findings of Meunier and Leweke.[4]

Introducing the nozzle structure into the flow causes a small increase in separation distance at all downstream locations. The corresponding reduction in rotation angle is not visible until $x/c=8$ is reached. For momentum coefficients $C_\mu=0.025$ and greater, merging is clearly delayed as two vortex structures exist even at $x/c=24$. An interesting observation is that between $x/c=8$ and 20, the gradients of all lines are approximately constant in Fig. 7(b). This indicates that the vortices approach each other at the same rate. The jet

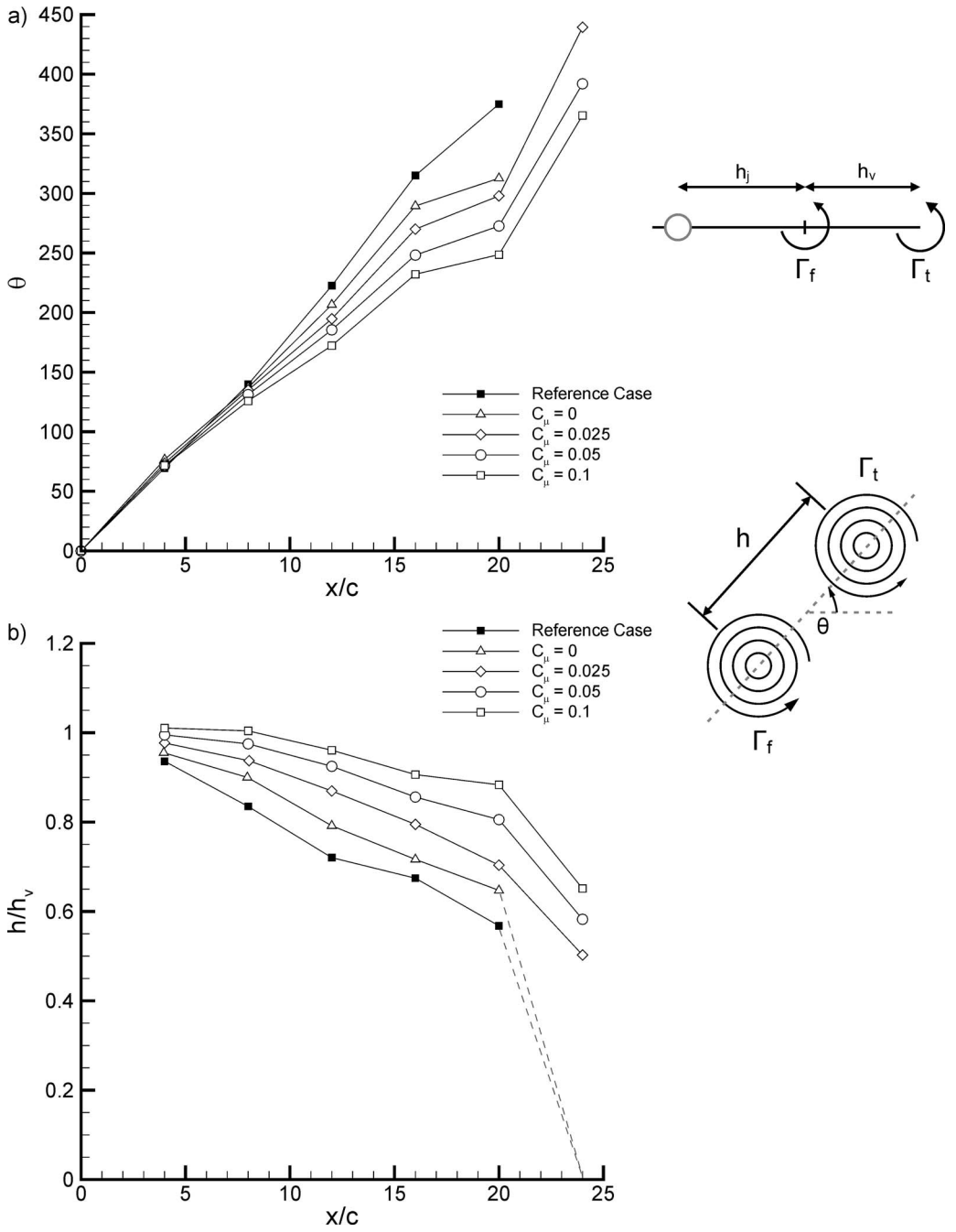

FIG. 7. Downstream development for equal strength corotating vortices for $h_v/c=0.75$ with the jet in configuration I (see schematic). (a) Time-averaged rotation angle and (b) time-averaged vortex separation.

flux has the greatest effect at the upstream locations where the gradients of the lines dramatically vary with blowing. The data indicate that the spacing remains approximately constant up to $x/c=8$, as the strength of the jet is raised. Even though the initial gradient of the lines varies, extrapolating the lines back to the ordinate axis suggests a convergence of the data at unity. Hence, the mechanism behind this could be interpreted as a delay in the onset of the convective stage. At $x/c=20$, the jet turbulence generated by a momentum flux of $C_\mu=0.1$ produced approximately a 63° reduction in rotation angle and a 40% increase in vortex spacing over the $C_\mu=0$ case.

Figure 8 suggests that moving the jet vertically below the flap has the exact opposite effect in which merging is promoted. Introducing the nozzle into the flow produces sufficient turbulence to cause an increase in rotation rate and a corresponding reduction in spacing. Merger now occurs upstream of $x/c=20$. In fact, increasing the momentum flux moves the merger point as far upstream as $x/c=12$ for $C_\mu=0.1$. There appears to be an increase in rotation angle for the blowing cases; however, this change is not as pronounced as for the horizontal jet. Another observation is that the gradients of the lines in Fig. 8(b) appear to become more negative as blowing increases. Physically, this means that the inward radial velocity of the vortex pair has increased. By extrapolating the data back to the ordinate axis, the lines tend

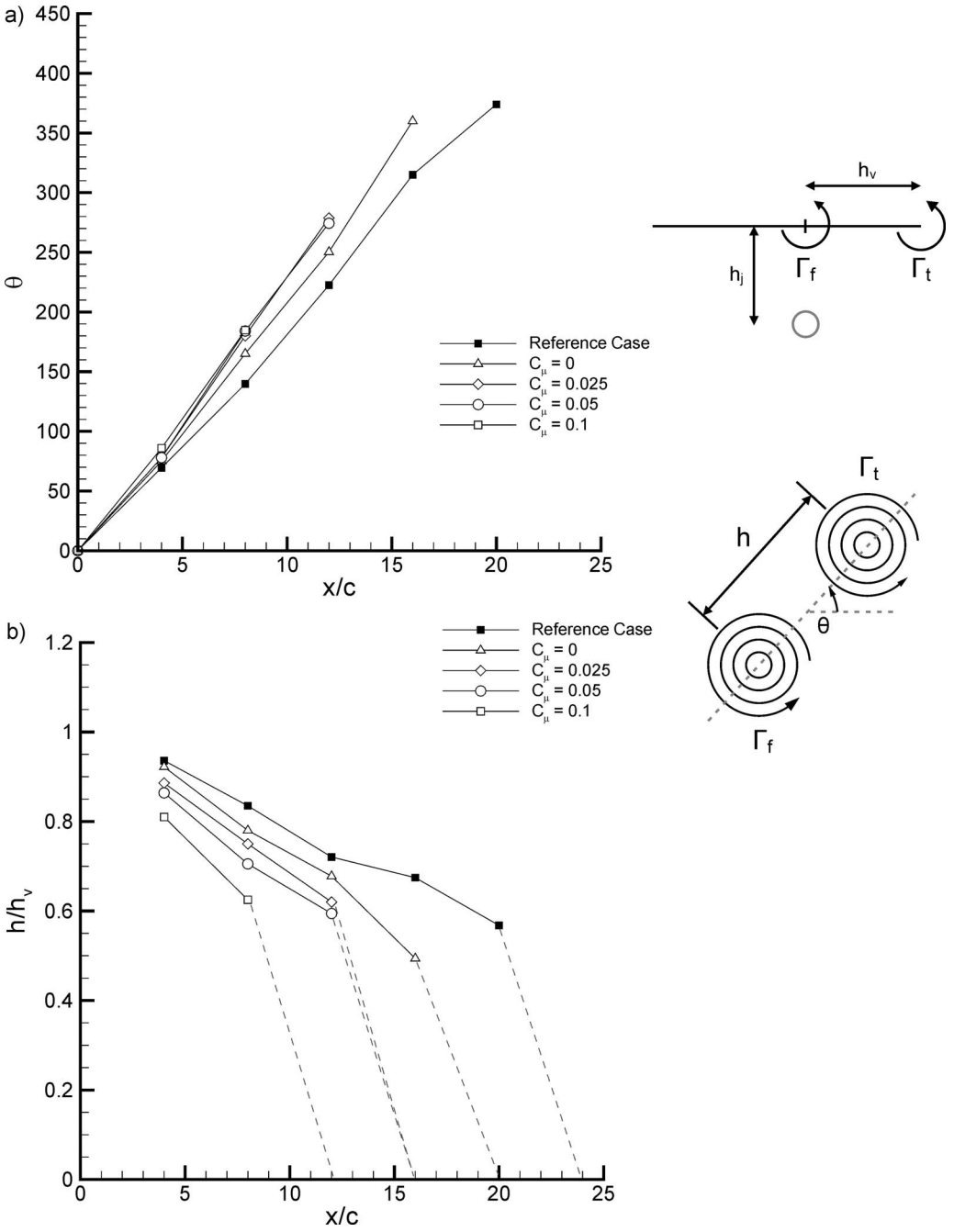

FIG. 8. Downstream development for equal strength corotating vortices for $h_v/c=0.75$ with the jet in configuration II (see schematic). (a) Time-averaged rotation angle and (b) time-averaged vortex separation.

to converge at nondimensional spacing of unity. Increasing the momentum coefficient to $C_\mu=0.1$ produces a 20% reduction in vortex spacing over the $C_\mu=0$ case at $x/c=8$. Analysis of the increase in area of the vortices as a result of merging does not reveal whether the jet turbulence has enhanced the production of the three-dimensional instabilities. The $C_\mu=0.05$ and 0.1 cases show an area increase of $(a_{\text{initial}}/a_{\text{final}})^2 \approx 4.0$ and 3.4, respectively, between $x/c=4$ and 20. It should be noted that the $C_\mu=0.05$ case has a larger area increase than the higher momentum coefficient because the final merged vortex was not fully axisymmetric.

So far, it has been shown that placing the jet in two different positions produces vastly dis-similar results. This suggests that the merging process is sensitive to the initial conditions. To analyze merging in detail, it is common for the velocity field to be transformed into a rotating frame. Figure 9 shows turbulence contours overlaid by streamlines at $x/c=4$ downstream and with $C_\mu=0.05$. By locating the nozzle $h_j/c=0.6$ horizontally inboard of flap [Fig. 9(a)], the jet turbulence clearly trails the flap vortex in close proximity, which disturbs the organized streamline patterns. This disturbance is located at the point where vorticity laden fluid from the inner region is advected to a larger radius by the rotation of the outer-recirculation region. Therefore, the jet has a major effect on the mechanism that produces convective merger. This idea can be used to aid the understanding of the trends

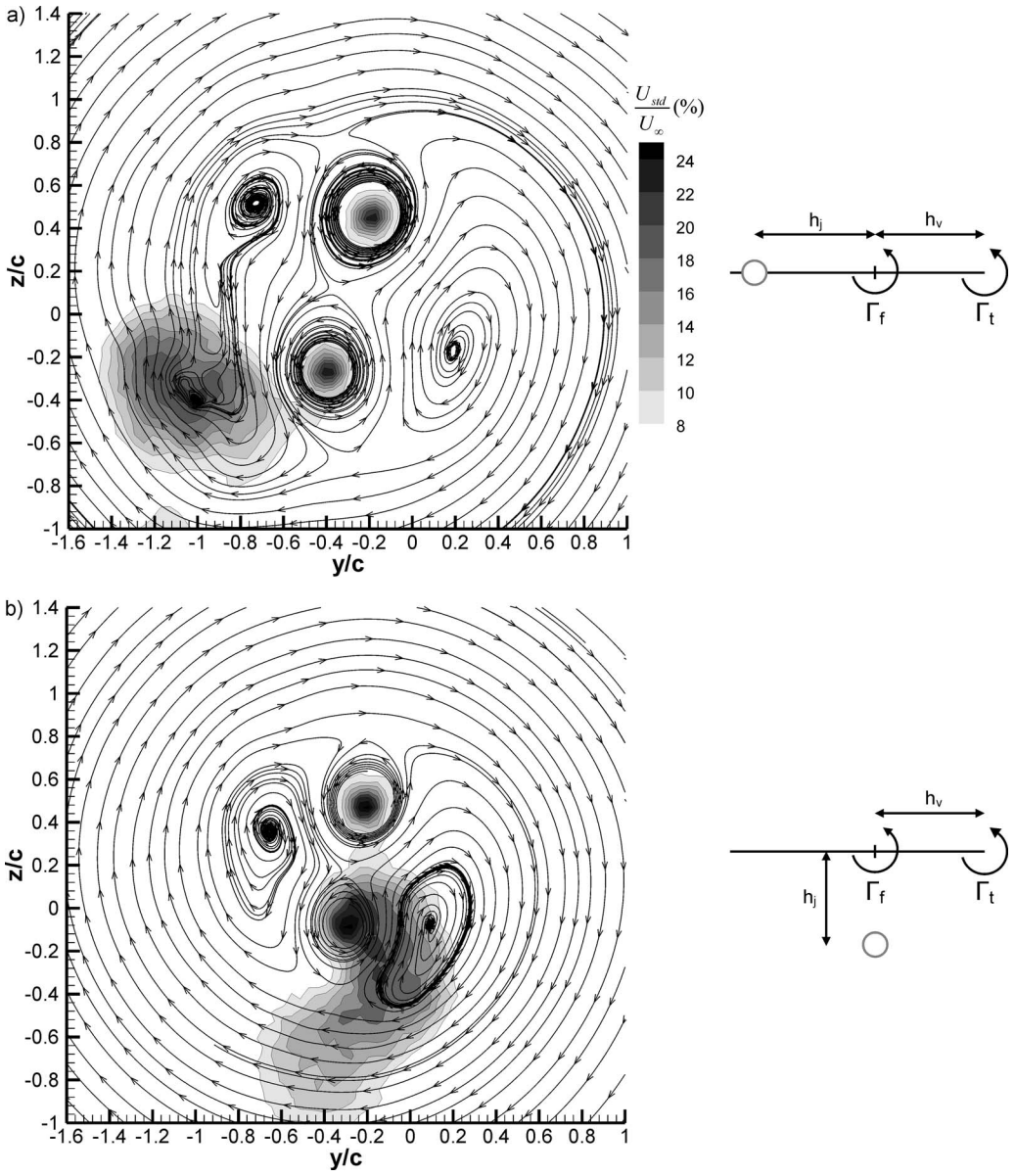

FIG. 9. Turbulence contours for equal strength corotating vortices overlaid with time-averaged streamlines in a rotating frame at $x/c=4$, $h_v/c=0.75$, $h_j/c=0.6$, and $C_\mu=0.05$. (a) Configuration I and (b) configuration II. Schematics indicate experimental setup.

produced in the vortex separation diagrams [Fig. 7(b)]. At upstream locations, where the jet turbulence intensity is still large, the gradient of the lines reduced, as previously discussed. Hence, the jet affects the convective stage, which impedes the approach of the vortex pair. As the turbulence decays or its position moves relative to the vortex pair, the outer-recirculation region regains its structure and ability to advect vorticity. Therefore, all lines have the same gradient [Fig. 7(b)] downstream of $x/c=8$ because the convective stage can proceed unaffected. Moving the jet to the vertical configuration in Fig. 9(b) does not appear to disrupt the streamlines. In this arrangement, high intensity jet turbulence directly interacts with the flap vortex, causing rapid diffusion.

Further experiments were performed at a larger initial vortex spacing of $h_v/c=1.0$. These data are useful because they will confirm whether the trends already discussed can be repeated with a different experimental arrangement. An additional jet location was included vertically below the center of the flap and tip, as seen in configuration III (Table II). This arrangement gives more information about the importance of the initial jet location.

Flow visualization in Fig. 10 was performed in exactly the same manner as previously seen. With the jet located at $0.6c$ inboard of the flap [Fig. 10(a)], similar results to those in Fig. 3 are produced at $x/c=4$. The jet fluid trails the flap vortex as the pair rotates due to their self-induced velocities. However, slightly more interaction was observed further downstream, probably because the rate of rotation is lower than in the previous case. Moving the jet vertically below the flap in Fig. 10(b) causes the bulk of the jet fluid to become elongated and stretched alongside the flap vortex. Further downstream, a severe interaction between the vortex pair and jet occurred. Finally, moving the jet vertically below the cen-

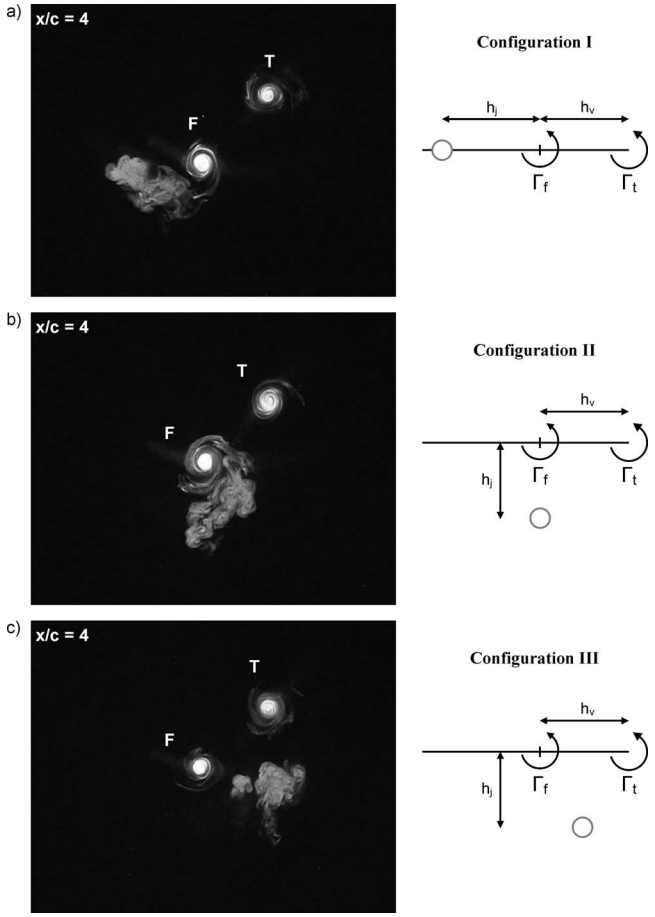

FIG. 10. Flow visualization for equal strength corotating vortices (T=tip vortex, F=flap vortex), $h_v/c=1.0$, $h_j/c=0.6$, and $C_\mu=0.025$. Schematics indicate experimental setup.

ter of the flap and tip (configuration III), as in Fig. 10(c), produces a different result. It might be expected to perform in a similar manner to configuration II [Fig. 10(b)] because the flap would still tend to rotate into the path of the jet. However, at $x/c=4$, no interaction with either vortex has occurred. This is similar to the horizontal case, except the jet fluid is now in the advancing side of the flap vortex. By analyzing the flow in the rotating reference frame for this case (Fig. 11), it is clear that the turbulence becomes encapsulated in the outer-recirculation region. This delays the interaction of the jet with either of the vortices.

By analyzing the vortex spacing for the $h_v/c=1.0$ experiments at $x/c=20$ in Fig. 12, it is clear that locating the jet vertically below the flap in configuration II provided the greatest promotion of merger compared to the other positions. This is because the jet causes a severe diffusion of the flap vortex, as previously seen in the $h_v/c=0.75$ case. The case with a jet momentum coefficient $C_\mu=0.1$ produced a single diffuse vortical structure that was approximately axisymmetric. Positioning the jet vertically below the center (configuration III) does slightly aid merging but only for larger momentum coefficients. This is likely to be because the interaction of the jet with the vortices is delayed as the jet fluid is located at the center of the outer-recirculation region. Finally, the horizontal case actually interferes and delays the merger process, consistent with previous findings. The change in spacing may not be as pronounced as the $h_v/c=0.75$ case but this is probably due to the reduced rotation rate of the vortex pair.

C. Unequal strength vortex merging

Merging of unequal strength corotating vortices is more representative of real aircraft wakes. Experiments have been performed with an initial vortex spacing $h_v/c=0.75$ and the jet in configurations I and II (Table II). During takeoff, the aircraft produces a pair of vortices with a relative strength $\Gamma_f<\Gamma_t$. The time-averaged velocity measurements revealed that the experimental setup generated an initial circulation ratio $\Gamma_f/\Gamma_t=0.65$. Figure 13 summarizes the separation distance as the vortex pair develops downstream. Results for configuration I [Fig. 13(a)] again indicate the occurrence of a delay to the merging process. Comparing $C_\mu=0$ and 0.1 at $x/c=16$ reveals an increase in separation distance of approximately 23%. A similar merging delay mechanism, as already seen for equal strength vortices, must be present. Figure 13(b) indicates that the results are again consistent with those already observed for cases where turbulence is introduced vertically below the flap (configuration II) because vortex separation is reduced.

Adapting the setup to simulate an approach configuration was achieved by increasing the strength of the flap vortex relative to the tip vortex. The circulation ratio measured in the wake at $x/c=4$ was $\Gamma_f/\Gamma_t=1.54$. Again, similar trends as previously observed for configurations I and II for an equal strength vortex pair were observed.

IV. CONCLUSIONS

This experimental study investigates the effect of a cold engine jet on the process of vortex merging in the near wake. Equal and unequal strength corotating vortices were produced to replicate the outboard flap-edge and wing-tip vortex structures generated by real aircraft. Flow visualization and particle image velocimetry measurements were performed to provide a detailed understanding of the jet effects on the vortical flow.

The sensitivity of vortex merging to the introduction of external turbulence has been revealed in this investigation. Severe effects on merging can occur if the turbulence interacts with the vortical structures before its intensity decays. The parameter that dictates whether merging will be promoted or delayed is the initial relative positions of the vortices and jet plume.

The largest promotion of merger occurs when the high intensity jet turbulence directly interacts with only one of the two vortices. This would occur on a four engined aircraft where the outboard jet is located vertically beneath the flap-edge vortex. Self-induced rotation of the vortex pair tends to directly move the flap vortex into the path of the exhaust plume. The consequence is a severe diffusion and reduction in coherency of the flap vortex. Merging is promoted as the flap vorticity begins to wrap around the unaffected and more concentrated tip vortex. The diffusion could also cause additional amounts of vorticity laden fluid from the flap vortex to

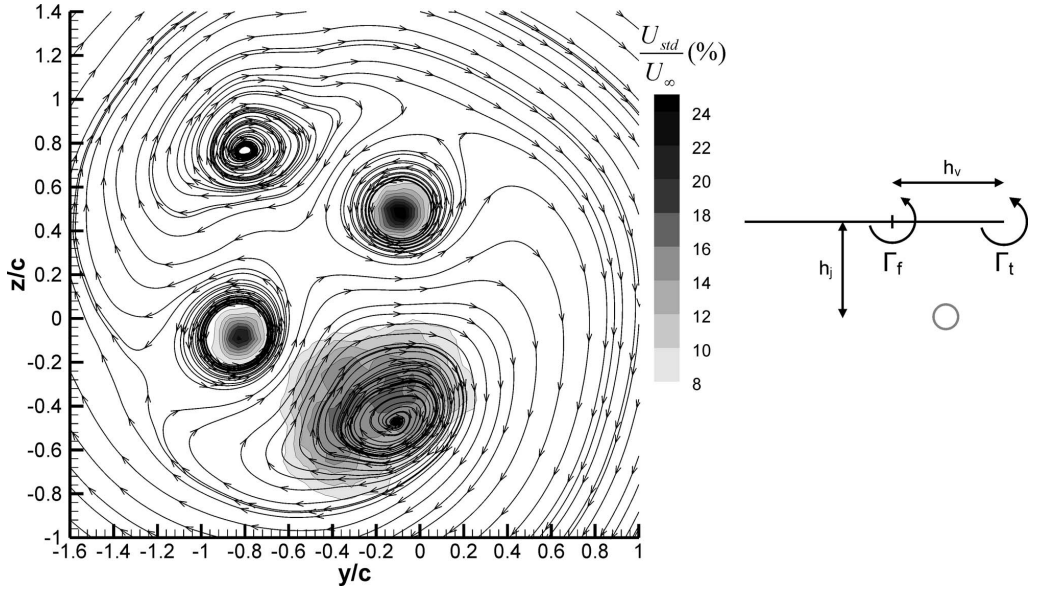

FIG. 11. Turbulence contours for equal strength corotating vortices overlaid with time-averaged streamlines in a rotating frame at $x/c=4$, $h_v/c=1.0$, $h_j/c=0.6$, and $C_\mu=0.05$ with the jet in configuration III (see schematic).

cross the separatrices into the outer-recirculation region. Advection of this fluid to a larger radius would result in the approach of the cores to conserve angular momentum. It is unclear from the current study whether the jet enhances the production of three-dimensional instabilities.

Repositioning the jet vertically beneath the center of the flap-edge and wing-tip vortices is again realistic of an outboard engine on a four engined aircraft. The rotational flow induced by the vortices tends to carry the jet fluid with the vortex pair, causing a more symmetric jet interaction and diffusion of both vortices. This does not leave a more concentrated vortex to dominate the merging process and consume the vorticity from the less coherent vortex structure. Merging was promoted but on a much smaller scale than previously seen. A small reduction in vortex spacing was observed which was likely to be facilitated by the transfer of vorticity across the rotating reference frame separatrices to the outer region where it can be advected outwards.

Locating the jet along the spanwise plane inboard of the flap is approximately representative of an aircraft with only two engines. It could be predicted that the jet fluid would directly interact with only the flap vortex, therefore, promoting merger. However, the results clearly indicate that the collapse of the vortex pair into a single structure is delayed. The analysis revealed that the jet turbulence tended to trail the flap vortex as the vortices rotated. Therefore, negligible in-

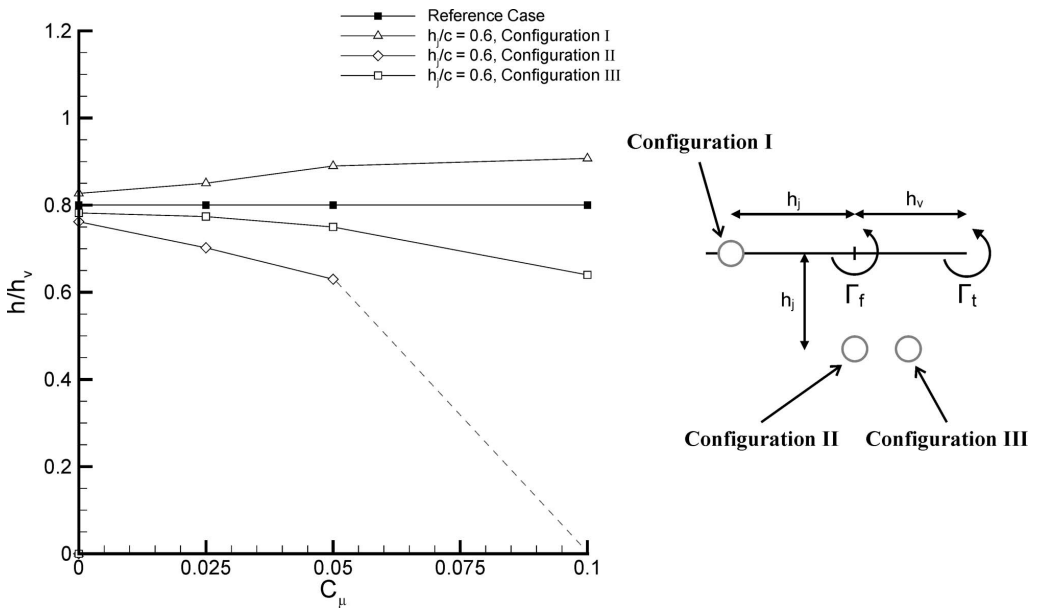

FIG. 12. Parametric analysis of time-averaged vortex separation as a function of momentum coefficient for equal strength corotating vortices at $x/c=20$, $h_v/c=1.0$, and $h_j/c=0.6$.

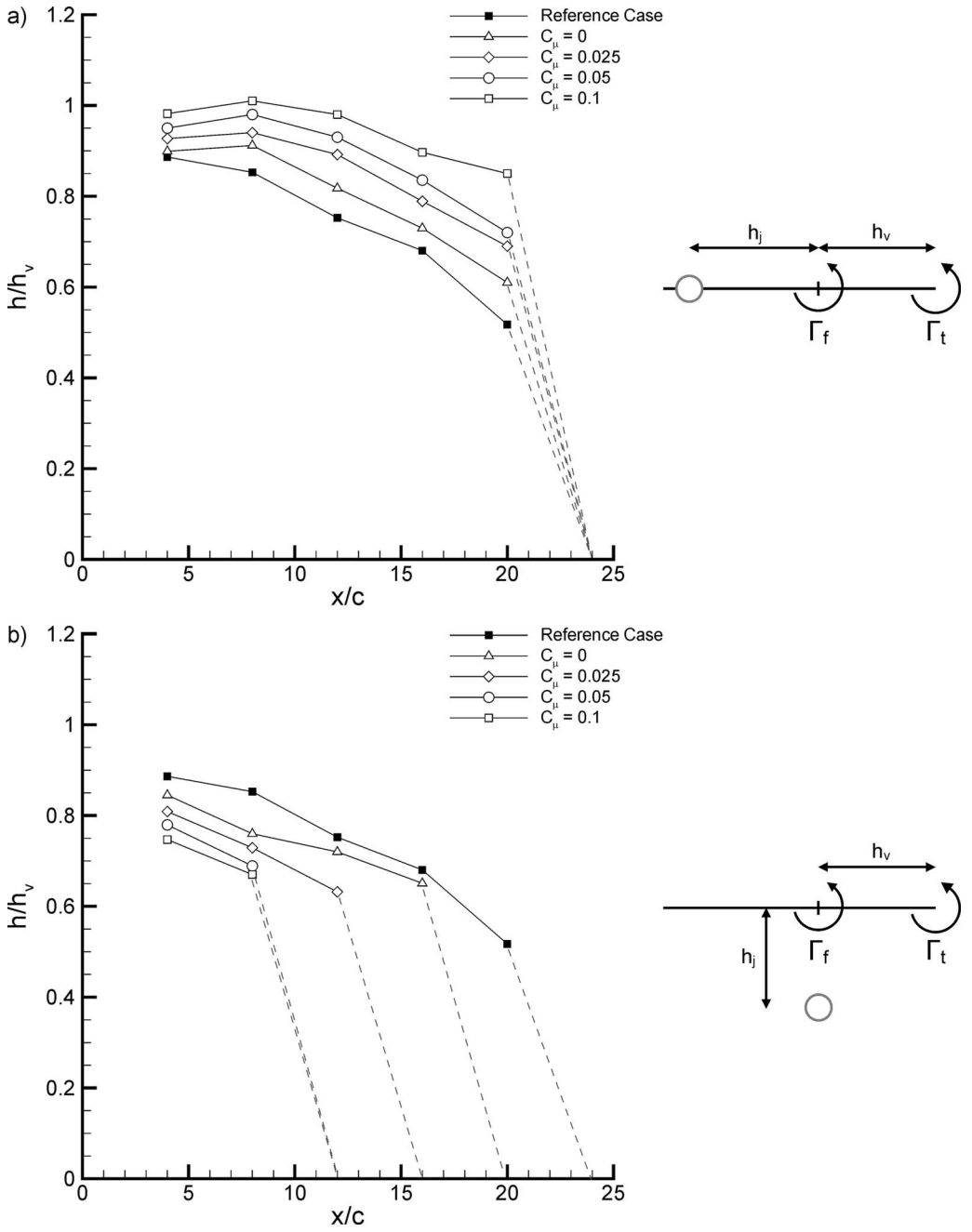

FIG. 13. Downstream development of time-averaged vortex separation for unequal strength corotating vortices ($\Gamma_f/\Gamma_t=0.65$) for $h_v/c=0.75$. (a) Jet in configuration I (see schematic) and (b) jet in configuration II (see schematic).

teraction between the jet fluid and the flap vortex was observed and the analysis revealed the jet flux to have little effect on the circulation of the vortices. However, the jet did cause a substantial increase in wandering of the flap vortex. The probable mechanism responsible for the delay was exposed when viewing the cross-flow rotating reference frame at the most upstream measurement location. The jet turbulence appears to alter the streamline pattern in the outer-recirculation region. The disturbance occurred at the point where vorticity is advected radially outward which clearly inhibits the convective merger stage, limiting its ability to reduce the separation of the vortex pair. Moving downstream results in a decay of the jet turbulence, allowing the outer-recirculation region to regain its coherence and, hence, the spacing of the vortex cores begins to reduce. Once the convective mechanism fully recovers, the approach velocity of the vortices is independent of the initial jet momentum coefficient.

The momentum flux was another parameter that was varied. Results revealed that the greater the strength of the jet is, the more turbulence that was introduced into the flow which consequently had a larger effect on the merging process. That is either more diffusion of the vortices or greater disruption to the outer-recirculation region. Similar trends were produced for all combinations of vortex circulation ratio, which are $\Gamma_f=\Gamma_t$, $\Gamma_f>\Gamma_t$, and $\Gamma_f<\Gamma_t$. Overall, it appears that the

data obtained on jet interactions with corotating vortices could be useful to alter the merging in the near wake for a real aircraft. This is especially true for takeoff when the jet flux from the engine is relatively large.

ACKNOWLEDGMENTS

This research has been performed with the support from European Commission Sixth Framework Programme Project, Fundamental Research on Aircraft Wake Phenomena (FAR-Wake).

[1] V. J. Rossow, "Lift-generated vortex wakes of subsonic transport aircraft," Prog. Aerosp. Sci. **35**, 507 (1999).
[2] P. Meunier, S. Le Dizes, and T. Leweke, "Physics of vortex merging," C. R. Phys. **6**, 431 (2005).
[3] A. L. Chen, J. D. Jacob, and O. Savas, "Dynamics of corotating vortex pairs in the wakes of flapped airfoils," J. Fluid Mech. **382**, 155 (1999).
[4] P. Meunier and T. Leweke, "Three-dimensional instability during vortex merging," Phys. Fluids **13**, 2747 (2001).
[5] C. Cerretelli and C. H. K. Williamson, "The physical mechanism for vortex merging," J. Fluid Mech. **475**, 41 (2003).
[6] T. Leweke, P. Meunier, F. Laporte, and D. Darracq, "Controlled interactions of co-rotating vortices," in *Third ONERA-DLR Aerospace Symposium (ODAS 2001)*, edited by K. Bütefisch *et al.* (ONERA, Paris, 2001), paper S2-3.
[7] R. W. Griffiths and E. J. Hopfinger, "Coalescing of geostrophic vortices," J. Fluid Mech. **178**, 73 (1987).
[8] P. Meunier, U. Ehrenstein, T. Leweke, and M. Rossi, "A merging criterion for two-dimensional co-rotating vortices," Phys. Fluids **14**, 2757 (2002).
[9] S. C. Crow, "Stability theory for a pair of trailing vortices," J. Fluid Mech. **8**, 2173 (1970).
[10] T. Leweke and C. H. K. Williamson, "Cooperative elliptic instability of a vortex pair," J. Fluid Mech. **360**, 85 (1998).
[11] J. Jimenez, "Stability of a pair of co-rotating vortices," Phys. Fluids **18**, 1580 (1975).
[12] R. Paoli and F. Garnier, "Interaction of exhaust jets and aircraft wake vortices: Small-scale dynamics and potential microphysical-chemical transformations," C. R. Phys. **6**, 525 (2005).
[13] G. K. Batchelor, "Axial flow in trailing line vortices," J. Fluid Mech. **20**, 645 (1964).
[14] R. Paoli, F. Laporte, B. Cuenot, and T. Poinsot, "Dynamics and mixing in jet/vortex interactions," Phys. Fluids **15**, 1843 (2003).
[15] A. Michalke and G. Hermann, "On the inviscid instability of a circular jet with external flow," J. Fluid Mech. **114**, 343 (1982).
[16] F. Y. Wang, M. M. J. Proot, J.-M. Charbonnier, and P. M. Sforza, "Near-field interaction of a jet with leading-edge vortices," J. Aircr. **37**, 779 (2000).
[17] F. Y. Wang and K. B. M. Q. Zaman, "Aerodynamics of a jet in the vortex wake of a wing," AIAA J. **40**, 401 (2002).
[18] P. Margaris, D. Marles, and I. Gursul, "Experiments on jet/vortex interaction," Exp. Fluids **44**, 261 (2008).
[19] D. G. Dritschel, "Strain-induced vortex stripping," in *Mathematical Aspects of Vortex Dynamics*, edited by R. E. Caflisch (SIAM, New York, 1989), pp. 107–119.